Bull. Mater. Sci., Vol. 39, No. 6, October 2016, pp. 1565–1568. © Indian Academy of Sciences.
DOI 10.1007/s12034-016-1303-y

Synthesis and characterization of multicolour fluorescent nanoparticles for latent fingerprint detection

G A SOBRAL Jr[1,2,*], M A GOMES[3], Z S MACEDO[3], M A R C ALENCAR[3] and S M V NOVAIS[3]

[1]Programa de Pós-Graduação em Materiais, Universidade Federal de Alagoas, Maceió, AL 57072-900, Brazil
[2]Instituto Federal de Alagoas, Rua Odilon Vasconcelos, 103, Jatiúca, Maceió, AL 57035-350, Brazil
[3]Departamento de Física, Universidade Federal de Sergipe, Cidade Universitária Prof. José Aloísio de Campos, Rod. Marechal Rondon s/n, Jardim Rosa Elze, São Cristóvão, SE 49100-000, Brazil

MS received 30 October 2015; accepted 15 April 2016

Abstract. **In this study, we successfully developed Y_2O_3 nanoparticles doped with Tb^{3+} and Eu^{3+} ions to generate fluorescent images of latent fingerprints. The optical and structural characterization of the nanoparticles was carried out and the fluorescence mechanisms are discussed. In our studies, the developed nanoparticles were effective in producing fluorescent images of latent fingerprints in shades of green, red and yellow with high-contrast colour under ultraviolet lighting.**

Keywords. **Fingerprint; nanocrystals; rare-earths; fluorescence.**

1. Introduction

The search for latent fingerprints at crime scenes is already a routine long present in the forensic science. Traditional materials used for this purpose usually just ensure a two tone contrast (clear/dark) between the latent fingerprints and background surfaces. This limitation hinders the work of forensic science technicians while analysing real-world scenarios, because such limited number of shades makes choosing the most appropriate powder a delicate task, in which, often, there will be no second chance. Another problem is the case with surfaces that presents colour gradient making it difficult to obtain images with the same consistent contrast over the entire surface [1,2]. As an alternative, fluorescent powders are used, which when spread over the latent fingerprints and exposed to a suitable source of light, emit a bright light thus facilitating the detection thereof. These powders typically use UV lights or a near-infrared laser as excitation source [3–5].

In this article, we developed yttria nanoparticles doped with rare-earth ions to produce fluorescent images of latent fingerprints under ultraviolet illumination. Due to the nano-sized dimension, low agglomeration and intense fluorescence shown by the developed nanoparticles, they are promising candidates for forensic applications, ensuring greater agility in latent fingerprint detection process due to the high fluorescent colour contrast presented by them and due to the variety of colours produced as a result of the use of different doping ions.

2. Experimental

The samples were produced via polyvinyl alcohol (PVA)-assisted sol–gel route, employing $Y(NO_3)_3$, $ErCl_3{\cdot}6H_2O$, $TbCl_3{\cdot}6H_2O$ and $Eu(NO_3)_3$ (Aldrich, grade purity 99.99% or higher) as precursors. For the Y_2O_3:Tb^{3+}, Y_2O_3:Eu^{3+} and Y_2O_3:Tb^{3+}-Eu^{3+} samples, dopant concentrations were fixed at 1 mol% each. Briefly, the starting materials were dissolved in distilled water in a concentration of 0.2 g ml^{-1}. After that, a 10% (w/v) aqueous solution of PVA was added to the starting solution under continuous stirring at room temperature. After 30 min stirring, the material was dried at 100°C for 24 h, then kept at 200°C for 5 h, and finally calcined at 1000°C for 5 h.

X-ray diffraction was used to determine the crystalline phase using a XRD (Rigaku RINT 2000/PC equipment), while morphology and particle size of the samples were analysed by scanning electron microscopy (SEM) using a Jeol JSM5500F equipment.

All Stokes luminescence spectra measurements under ultraviolet light excitation were performed using a Jobin Yvon™ Fluorolog® 3 spectrofluorometer with excitation and emission slits adjusted to 1 nm.

For the preparation of the fingerprints, the index finger was pressed against the surface of a clean glass slide. Over the remaining fingerprint, nanoparticles were sprinkled and excess powder was removed gently with a brush.

*Author for correspondence (geraldo@optma.org)

The pictures of the fingerprints were taken using a Canon PowerShot SX510 HS digital camera in automatic mode positioned at a distance of 15 cm just above the samples. In front of the camera lens was placed a UV-cut filter (blocking below 400 nm) to avoid exposure to residual light of the excitation source. While fingerprints were photographed, the excitation wavelength was set at 310 nm for Y_2O_3:Tb^{3+} and Y_2O_3:Tb^{3+}-Eu^{3+} samples, and at 260 nm for Y_2O_3:Eu^{3+} sample. The excitation of the samples by UV source was done at an angle of 45°. All measurements were performed at room temperature.

3. Results and discussion

3.1 *Structure and morphology of the synthesized material*

Figure 1 shows XRD pattern of Y_2O_3:Tb^{3+}-Eu^{3+} co-doped sample. The found diffraction peaks are in conformity with the ICSD card (#086817) for the cubic phase of Y_2O_3 to all the samples studied. The Rietveld refinement of the pattern confirmed a cubic structure and revealed that the low concentration of dopants used (1 mol% each) did not significantly affect the lattice parameters, which were 10.6008 Å for Y_2O_3:Eu^{3+} sample, 10.5960 Å for Y_2O_3:Tb^{3+} sample and 10.5972 Å for Y_2O_3:Tb^{3+}-Eu^{3+} co-doped sample.

The crystallite size was estimated from the full-width half-maximum of the diffraction peaks using Scherrer's equation $d = K\lambda/\beta \cdot \cos\theta_B$, with parameters defined as usual [6]. In this work $K = 0.89$, $\lambda = 0.15405$ nm, θ_B is the peak position and $\beta = \sqrt{B^2 - b^2}$ is the width of specimen's peak (B) corrected by an instrumental broad factor (in this work, $b = 0.005192$ rad) [6,7]. The average crystallite size was estimated as 43 ± 1 nm. Figure 2 presents SEM image of the powders, where the average particle size is about 50 nm.

3.2 *Fluorescence of the nanoparticles*

Figure 3 shows the fluorescence spectra for each studied sample. Unfortunately it was not possible to record the emission of the sample in some regions (indicated in figure) due to the inability to filter the second-order term signal from the excitation lamp, but this minor inconvenience did not affect our analysis.

By analysing the emission spectra presented in figure 3, it becomes clear that the sample doped with Tb^{3+} ions must present predominantly green colour due to their most intense emission bands centred at 490 and 550 nm, because of the transitions from $^5D_4$ level to ^7F_J level in ions of terbium [8–11], while the sample doped with Eu^{3+} has its most intense emission band centred at 611 nm resulting in the characteristic red colour of this phosphor due to transitions from $^5D_0$ level to $^7F_2$ level [12]. Finally, by doping the same sample with the two ions (Tb^{3+} and Eu^{3+}), as we might expect, we obtain a yellowish phosphor due to the combination of green and red bands already identified previously. In this case, we suppose that the excitation with 310 nm occurs

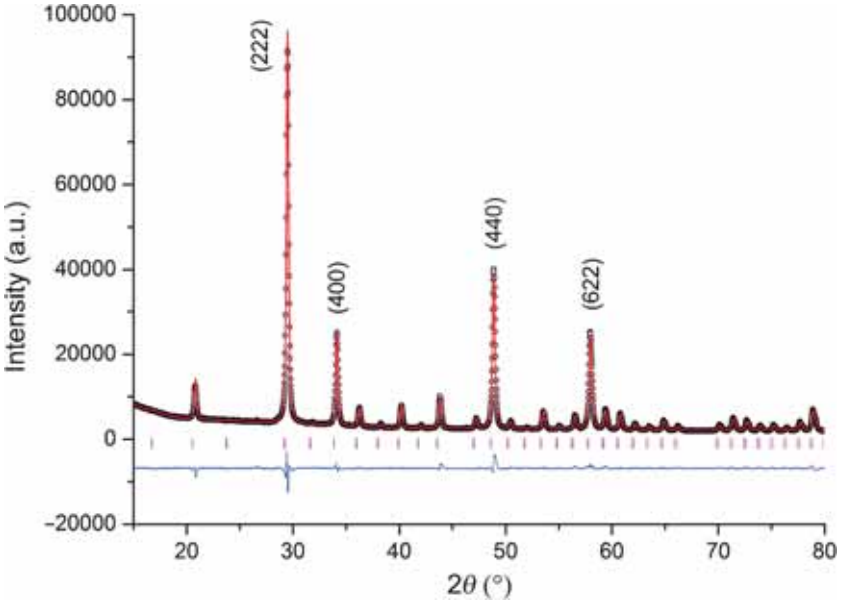

Figure 1. Rietveld refinement of Y_2O_3:Tb^{3+}-Eu^{3+}. Open circles represent the XRD data and the solid curve represents the calculated pattern. Difference plot is shown at the bottom of the graph.

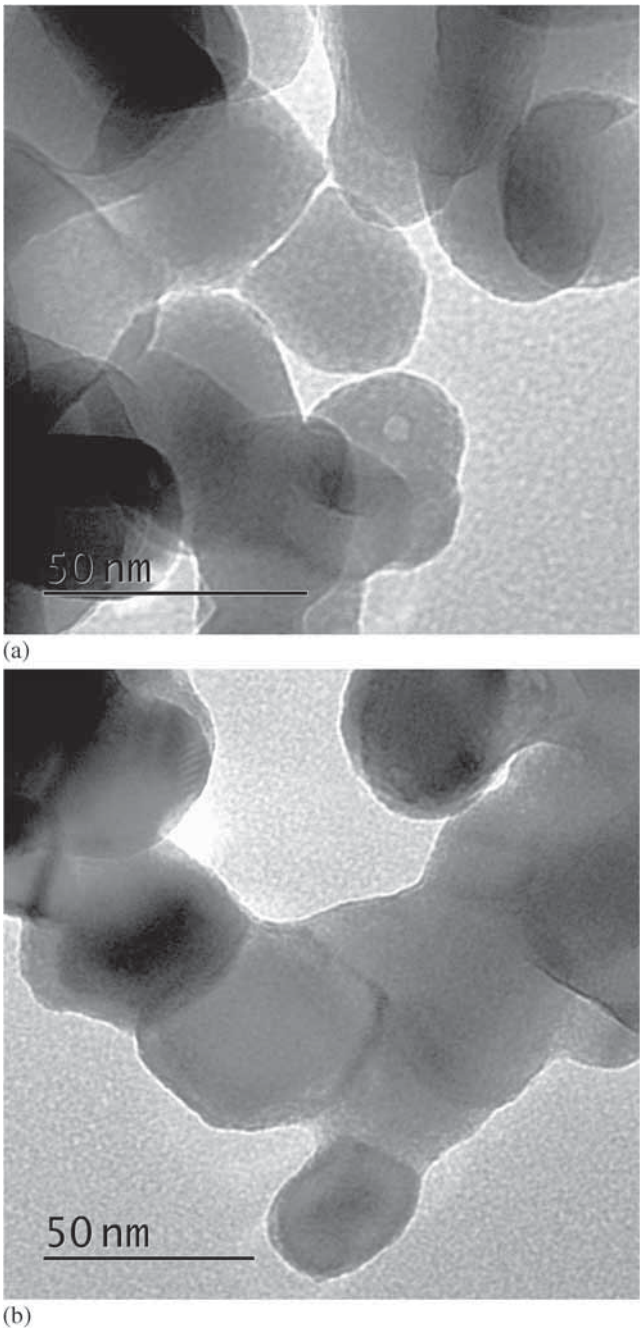

Figure 2. SEM image of (**a**) Y_2O_3:Tb^{3+} and (**b**) Y_2O_3:Tb^{3+}-Eu^{3+} samples, with average particle size of about 50 nm.

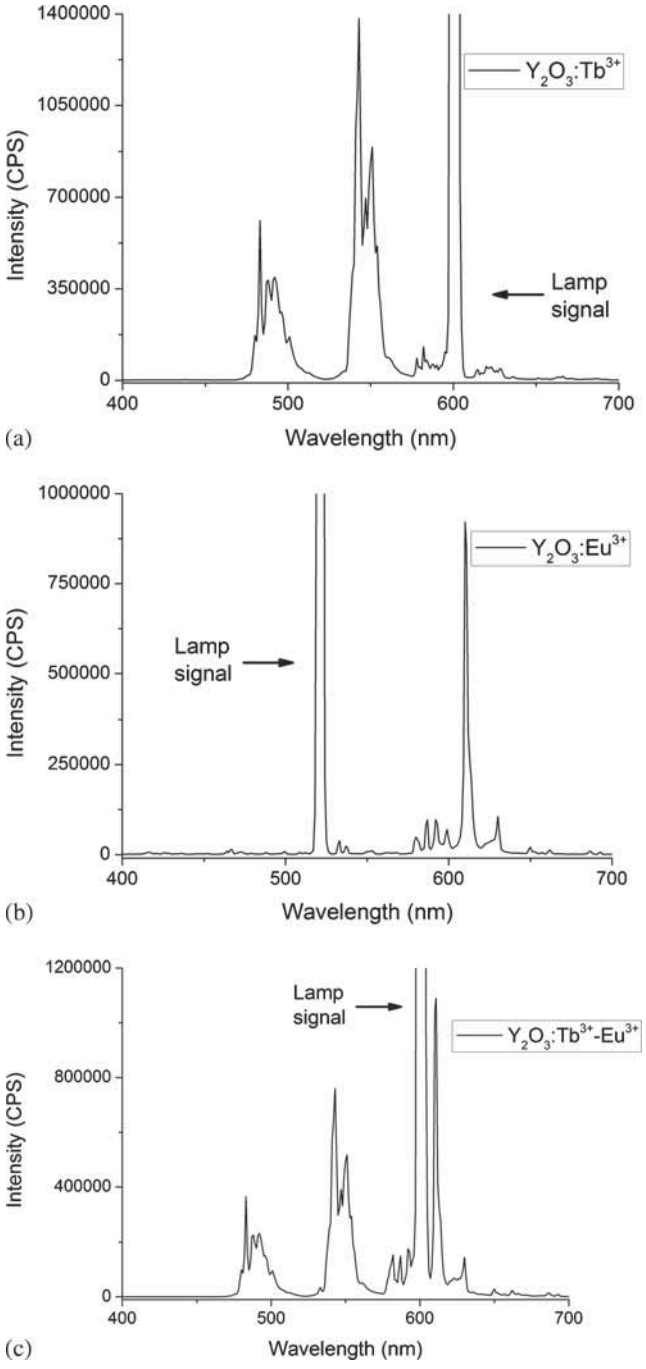

Figure 3. Emission spectra of Y_2O_3 samples under UV excitation. (**a**) Tb^{3+}-doped sample under 310 nm excitation, (**b**) Eu^{3+}-doped sample under 260 nm excitation and (**c**) Tb^{3+}-Eu^{3+}-doped sample under 310 nm excitation.

predominantly on the terbium ions, which act as a sensitizer transferring energy to europium ions. As suggested in other studies, this energy transfer from Tb^{3+} to Eu^{3+} ions occurs through a non-resonant cross-relaxation process followed by absorption of phonons from the host matrix [13], the exchange of energy in the opposite direction $Eu^{3+} \rightarrow Tb^{3+}$ is negligible [14].

Finally, we analysed the performance of the nanoparticles by sprinkling them onto glass slides containing fingerprints previously produced. These glass slides were exposed to ultraviolet light of the same wavelength used for the determination of fluorescent emission spectra in figure 3. The results are shown in figure 4.

As can be seen in figure 4, the developed fluorescent nanoparticles fit perfectly to the subtleties of the fingerprint lines, clearly outlining the contours thereof and also maintaining intense fluorescence intensity that can be easily seen by the naked eye.

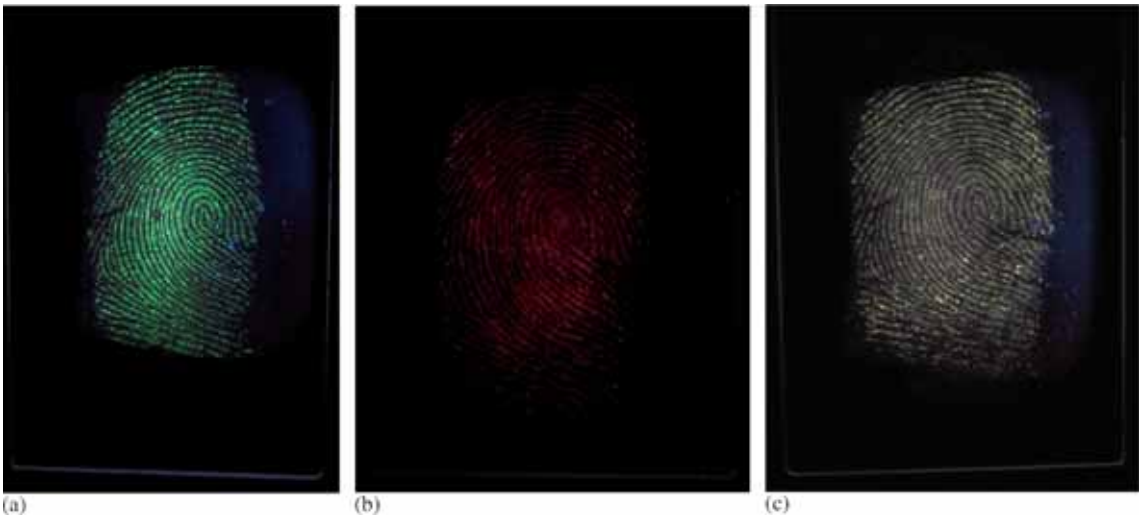

Figure 4. Fluorescent fingerprints obtained by sprinkling the developed nanoparticles on latent fingerprints on glass slides, followed by UV excitation of them. (**a**) Green fluorescence obtained from Y_2O_3:Tb^{3+} sample, (**b**) red fluorescence obtained from Y_2O_3:Eu^{3+} sample and (**c**) yellowish fluorescence obtained from Y_2O_3:Tb^{3+}-Eu^{3+} sample.

4. Conclusions

We carried out the synthesis of Y_2O_3 fluorescent nanoparticles doped with Tb^{3+} and Eu^{3+}, performing its morphological and structural characterization and analysing their fluorescence mechanisms under UV excitation. Finally, we showed that these nanoparticles can be effectively used for detection of latent fingerprints, facilitating detection of these impressions based on the fluorescent properties exhibited by the nanoparticles and increasing the contrast between the fingerprints and the surfaces on which they lay. For all of that, the developed nanoparticles are promising candidates for real forensic applications.

Acknowledgements

We acknowledge CAPES, CNPq, FINEP and FAPITEC/SE for the financial support, and CMNano-UFS for microscopy facilities.

References

[1] Saferstein R 1978 *Criminalistics: an introduction to forensic science* (New Delhi: Prince-Hall) p 279

[2] Sodhi G S and Kaur J 2001 *Forensic Sci. Int.* **120** 172

[3] Wang M, Li M, Yang M, Zhang X, Yu A, Zhu Y, Qiu P and Mao C 2015 *Nano Res.* **8** 1800

[4] Pandey A and Rai V K 2012 *Appl. Phys. B* **109** 611

[5] Liu L, Gill S K, Gao Y, Hope-Weeks L J and Cheng K H 2008 *Forensic Sci. Int.* **176** 163

[6] Cullity B D 1978 *Elements of X-ray diffraction* (Massachusetts: Addison-Wesley) p 99

[7] Gomes M A, Valerio M E G and Macedo Z S 2011 *J. Nanomater.* 469685 1

[8] Back M, Massari A, Boffelli M, Gonella F, Riello P, Cristofori D, Riccò R and Enrichi F 2012 *J. Nanopart. Res.* **14** 792

[9] Duhamel-Henry N, Adam J L, Jacquier B and Linarès C 1996 *Opt. Mater.* **5** 197

[10] Robbins D J, Cockayne B, Lent B and Glasper J L 1976 *Solid State Commun.* **20** 673

[11] Berdowski P A M, Lammers M J J and Blasse G 1985 *Chem. Phys. Lett.* **113** 387

[12] Tallant D R, Seager C H and Simpson R L 2002 *J. Appl. Phys.* **91** 4053

[13] Kim Anh T, Ngoc T, Thu Nga P, Bitch V T, Long P and Strek W 1988 *J. Luminescence* **39** 215

[14] Mukherjee S, Sudarsan V, Vatsa R K, Godbole S V, Kadam R M, Bhatta U M and Tyagi A K 2008 *Nanotechnology* **19** 325704